

See discussions, stats, and author profiles for this publication at: <https://www.researchgate.net/publication/350122413>

Bioactive compounds from Octopus vulgaris ink extracts exerted anti-proliferative and anti-inflammatory effects in vitro

Article in *Food and Chemical Toxicology* · March 2021

DOI: 10.1016/j.fct.2021.112119

CITATIONS

18

READS

431

11 authors, including:



[Martin Samuel Hernandez Zazueta](#)

Universidad de Sonora (Unison)

8 PUBLICATIONS 62 CITATIONS

[SEE PROFILE](#)



[Ivan Luzardo-Ocampo](#)

Tecnológico de Monterrey

75 PUBLICATIONS 884 CITATIONS

[SEE PROFILE](#)



[Joel Said García-Romo](#)

Universidad Estatal de Sonora

9 PUBLICATIONS 72 CITATIONS

[SEE PROFILE](#)



[Luis Noguera-Artiaga](#)

Universidad Miguel Hernández de Elche

66 PUBLICATIONS 1,148 CITATIONS

[SEE PROFILE](#)



Bioactive compounds from *Octopus vulgaris* ink extracts exerted anti-proliferative and anti-inflammatory effects *in vitro*

Martín S. Hernández-Zazueta^a, Iván Luzardo-Ocampo^{b,c}, Joel S. García-Romo^a, Luis Noguera-Artiaga^d, Ángel A. Carbonell-Barrachina^d, Pablo Taboada-Antelo^e, Rocío Campos-Vega^b, Ema Carina Rosas-Burgos^a, María G. Burboa-Zazueta^f, Josafat M. Ezquerra-Brauer^a, Armando Burgos-Hernández^{a,*}

^a Departamento de Investigación y Posgrado en Alimentos, Universidad de Sonora, 1658, Hermosillo, Sonora, Mexico

^b Research and Graduate Program in Food Science, School of Chemistry, Universidad Autónoma de Querétaro, 76010, Querétaro, Qro, Mexico

^c Instituto de Neurobiología, Universidad Nacional Autónoma de México, 76230, Juriquilla, Qro, Mexico

^d Escuela Politécnica Superior de Orihuela, Universidad Miguel Hernández de Elche, 03312, Alicante, Spain

^e Departamento de Física Aplicada, Universidad de Santiago de Compostela, 15782, Santiago de Compostela, Spain

^f Departamento de Medicina y Ciencias de la Salud, Universidad de Sonora, 83000, Hermosillo, Sonora, Mexico

ARTICLE INFO

Handling Editor: Dr. Jose Luis Domingo

Keywords:

Octopus (*Octopus vulgaris*)
Anti-proliferative effect
Cytokine modulation
Colorectal cancer
Ink
Metabolomic analysis

ABSTRACT

Underutilized marine food products such as cephalopods' ink could be sources of bioactive compounds providing health benefits. This study aimed to assess the anti-proliferative and anti-inflammatory effects from *Octopus vulgaris* ink extracts (hexane-, ethyl acetate-, dichloromethane- (DM), and water extracts) using human colorectal (HT-29/HCT116) and breast (MDA-MB-231) cancer cells, and LPS-challenged murine RAW 264.7 cells. Except by ethyl-acetate, all of the extracts exhibited anti-proliferative effects without being cytotoxic to ARPE-19 and RAW 264.7 cells. Among DM fractions (F1/F2/F3), DM-F2 showed the highest anti-proliferative effect ($LC_{50} = 52.64 \mu\text{g/mL}$), inducing pro-apoptotic morphological disruptions in HCT116 cells. On RAW 264.7 cells, DM-F2 displayed the lowest nitrites reduction and up-regulation of key-cytokines from the JAK-STAT, PI3K-Akt, and IL-17 pathways. Compared to control, DM-F2 increased IL-4 and decreased NF-κB fluorometric expression in peripheral blood mononuclear cells (PBMCs). Metabolomic analysis of DM-F2 highlighted hexadecanoic acid and 1-(15-methyl-1-oxohexadecyl)-pyrrolidine as the most important metabolites. These compounds also exhibited high *in silico* binding affinity (-4.6 to -5.8 kcal/mol) to IL-1 α , IL-1 β , and IL-2. Results suggested the joint immunomodulatory and anti-proliferative effect derived from selected compounds of underutilized marine food products such as ink. This is the first report of such biological activities in extracts from *O. vulgaris* ink.

1. Introduction

Cancers have been responsible for more than 18 million dead worldwide, being lung (11.58%), breast (11.55%), colorectal (10.23%), prostate (7.06%), and stomach (5.72%) the most common types of this disease (IARC, 2018). Approximately 25% of all cancers are associated with inflammatory processes, and 15% of the derived deaths are estimated to have been linked to them (Allavena et al., 2008; Coussens and Werb, 2002). Within cancer processes, pro-inflammatory molecules, such as cytokines and chemokines, inducible nitric oxide synthase (iNOS), reactive oxygen species (ROS), and nuclear factor-kappa B

(NF-κB) are upregulated (Sarkar and Fisher, 2006). Although the resulting pro-inflammatory response could generate an adverse outcome, intense immune cell infiltration is associated with improved survival due to the recognition of transformed malignant cells, restricting tumor growth (Tuomisto et al., 2019).

Conventional treatments such as chemotherapy and radiotherapy have been extensively used in most cases with locally advanced or systemic metastasis, with no major improvements in their prognosis (Sun et al., 2020). Regarding chemotherapy, the drugs used arrest the cell cycle, affecting both active mitotic cancer cells and the proliferation of normal non-cancerous-fast growing cells (bone marrow, hair follicles, or cells from the digestive system), producing side effects (Mitchison,

* Corresponding author. Departamento de Investigación y Posgrado en Alimentos, Universidad de Sonora, Apartado Postal 1658, 83000, Hermosillo, Sonora, Mexico.

E-mail address: armando.burgos@unison.mx (A. Burgos-Hernández).

Abbreviations	
AGE-RAGE	Advanced glycation end-products receptor for AGE
AMC	Analysis of major components
BCA	Bicinchoninic acid
DAPI	4'6'-diamidino-2-phenylindole-tetramethylrhodamine B isothiocyanate
DM	Dichloromethane extract from <i>Octopus vulgaris</i> ink
DM-F1, F2, F3	Fraction 1, 2, 3 from DM extract
DMEM	Dulbecco's modified eagle medium
EA	Ethyl acetate extract from <i>O. vulgaris</i> ink
FA	Fatty acid
FBS	Fetal bovine serum
FceR1	FCe receptor 1
FDR	False discovery rate
FITC	Fluorescein isothiocyanate
GC-MS	Gas-chromatography
KEGG	Kyoto Encyclopedia of Genes and Genomes
H2DCFDA	2',7'-dichlorodihydrofluorescein diacetate
HDFs	Human dermal fibroblasts
HX	Hexane extract from <i>O. vulgaris</i> ink
IBD	Inflammatory bowel disease
IC50	Half inhibitory concentration
iNOS	Inducible nitric oxide synthase
JAK-STAT	Janus kinase-signal transducer and activator of transcription
LC-ESI-Q	Liquid chromatography coupled to quantitative
LPS	electrospray ionization
MDA	Lipopolysaccharides from <i>Escherichia coli</i> O111:B4
MIC80	Malonaldehyde
MS	80% minimal inhibitory concentration
MTT	mass spectrometry analysis
	3-(4,5-dimethylthiazol-2-yl)-2,5-diphenyltetrazolium bromide;
ND	Non-detected
NF-κB	Nuclear factor κB
PBMCs	Peripheral blood mononuclear cells
PI3K	Phosphatidylinositol-3-kinase pathway
PLS-DA	Partial least-squares discriminant analysis
RFU	Relative fluorescence units
RI (exp.)	Experimental retention index
RI (rep.)	Reported retention index
ROS	Reactive oxygen species
RT	Room temperature (25 ± 1 °C)
SDS	Sodium dodecyl sulfate
sICAM-1	Soluble forms of intercellular adhesion molecule 1
SOD	Superoxide dismutase
TH	T-helper cells
TLC	Thin-layer chromatography
TLP	Thin-layer plate
TRAIL	TNF-related apoptosis-inducing signal
VIP	Variable Importance in Projection
WE	Water extract from <i>O. vulgaris</i> ink

2012). Hence, more adequate strategies should be researched, aiming to reduce negative effects.

Cancer development is highly associated with risk factors such as lifestyle choices and diet (Mysuru Shivanna and Urooj, 2016). Therefore, targeting anti-inflammatory bioactive compounds from natural products has emerged as an integrative approach of the cancer condition (Ammendola et al., 2020). Secondary metabolites from the wide variety of marine fauna flora could be a natural source of these type of compounds with unlimited diverse biological properties (Barzkar et al., 2019; Malve, 2016). Among these properties, cancer treatment and prevention have been extensively reported (Khalifa et al., 2019). For instance, marine products have shown tumor autophagy regulation via PI3K/Akt/mTOR, p53, and up-regulation of activated c-Jun N-terminal kinase (JNK) signaling (Wargasetia and Widodo, 2019). On the other hand, cephalopod ink has displayed potential as an anticancer agent *in vitro*, but its specificity on certain cancer cells has not been fully explored (Fahmy and Soliman, 2013; Naraoka et al., 2000). Even more, few reports have assessed the anti-inflammatory properties of the ink or its relationship with the development of cancer (Derby, 2014). However, there are reports regarding the antimicrobial potential of peptides (OctoPartenopin) from *O. vulgaris*' suckers, evidenced in the inhibition of known microorganisms such as *Staphylococcus aureus*, *Pseudomonas aeruginosa*, and *Candida albicans* (Maselli et al., 2020) and the antimicrobial activity of specific cell types like hemocytes, also showing high inhibitory activity on *Bacillus cereus*, *Listeria monocytogenes*, and *S. aureus*, among other bacterial strains (Troncone et al., 2015).

Our research group previously reported the antioxidant, anti-mutagenic, cytoprotective, anti-proliferative, and pro-apoptotic effects of octopus' ink fractions on selected human cancer cell lines (A549, HeLa, and 22Rv1) (Hernández-Zazueta et al., 2021), but no anti-inflammatory mechanisms nor their effects on colorectal cells was explored. Thus, the present study aimed to evaluate the anti-proliferative effect from *Octopus vulgaris* ink extracts *in vitro* using selected human cancer cell lines (HCT116, HT-29, and MDA-MB-231), as well as its anti-inflammatory effects on both, human peripheral

blood mononuclear cells (PBMCs) and murine cell line (RAW 264.7). Human retinal pigmented epithelial cells (ARPE-19) were used as a control for cytotoxicity based on previous research using these cells for such a purpose (Lord et al., 2019; Weng et al., 2017).

2. Materials and methods

2.1. Preparation of *O. vulgaris* ink extracts and fractions

O. vulgaris specimens captured by local fishermen at shallow water of Kino Bay, Sonora, Mexico ($29^{\circ}2227$ N, $112^{\circ}3408$ W) were transported in ice to the laboratory where they were processed. Briefly, 1.30 Kg of octopus wastes were collected, from which 20 sacs were obtained as discard material from the octopus. The ink was extracted from sacs, as reported by Ebada et al. (2008). Afterward, 15 mL of the ink were homogenized with HPLC-grade water (1:1 ratio) and freeze-dried (Labconco Corp., Kansas City, MO, US). Four extracts were prepared from the resulting freeze-dried mixture: hexane- (HX), ethyl acetate- (EA), dichloromethane- (DM), and water-soluble (WE) extracts. Since the DM further exhibited the highest anti-proliferative potential after the initial screening with the cancerous cell-lines, purified DM fractions were generated. For this, the DM extract was dissolved in ethyl acetate and fractioned in silica gel columns (3.5 cm × 60 cm, 60–120 mesh silica gel; Sigma-Aldrich, St. Louis, MO, US). The elution was conducted using hexane: ethyl acetate (99:1) as a mobile phase, producing 25 mL-fractions. A total of 38 fractions were obtained, and those with similar contents (monitored by thin-layer chromatography, TLC) were mixed to obtain the F1, F2, and F3 fractions from DM. For the semipreparative TLC, DM fractions were applied onto silica (F₂₅₄, 0.040–0.043 mm; Merck, Kenilworth, NJ, US) pre-coated TLC plate and developed under a 95:5 hexane:ethyl acetate (v/v) mobile phase (Liu et al., 2008). The TLC plate was UV-monitored to determine the composition of the eluted fractions. The fractions were evaporated under vacuum and dried with nitrogen.

2.2. Analysis of volatile compounds of DM and DM-F2 extracts by gas chromatography/mass spectrometry (GC-MS)

The analysis of volatile compounds of the bioactive fraction DM and DM-F2 was determined by gas chromatography coupled to mass spectrometry (GC-MS) (Noguera-Artiaga et al., 2019) using a Shimadzu GC-17A coupled to a Shimadzu QP-5050 mass detector system (Shimadzu Corporation, Kyoto, Japan). The GC-MS was equipped with an SLB-5ms Capillary GC Column (30 m × 0.25 mm, 0.25 µm, Supelco Inc, Sigma-Aldrich). Helium was used as carrier gas at a flow rate of 0.6 mL/min in a splitless mode. The oven temperature started at 80 °C and, after 5 min of stabilization, it was increased by 2 °C/min up to 220 °C. After 5 min of stabilization, the temperature was increased by 25 °C/min up to 300 °C, and it was held for 1.80 min. Detector and injector temperatures were 300 and 230 °C, respectively. The compounds were identified using 3 analytical methods: retention indexes, GC-MS retention indexes, and mass spectra (NIST05 and WILEY229 spectral libraries' collection) analyses. The identification was considered tentative when it was based only on mass spectral data. The results were expressed as a percentage of the total area represented by each one of the compounds.

2.3. Untargeted metabolomic analysis

A global and untargeted metabolomic analysis was conducted for the identified metabolites from DM and DM-F2 using GC-MS (Gertsman and Barshop, 2018). All data were normalized using the MetaboAnalyst 3.0 software. Analysis of major components (AMC) was used to observe the patterns of metabolites from each sample. A partial least square discriminant analysis (PLS-DA) was used to rank each metabolite from the samples according to the number of components and variables of each model (Lê Cao et al., 2011). The variable importance in projection (VIP) scores were obtained for classifying the importance of each metabolite based on its discrimination rule of importance (VIP ≥ 2) (RoyChoudhury et al., 2017).

2.4. Cell culture

The human colorectal carcinoma HCT116 (ATCC® CCL-247™), colorectal adenocarcinoma HT-29 (ATCC® HTB-28™), mammary gland/breast adenocarcinoma MDA-MB-231 (ATCC® HTB-26™) and murine macrophages RAW 264.7 (ATCC® TIB-71™) were acquired from American Type Culture Collection (Manassas, VA, US.). The cells were cultured under proper conditions (37 °C, humidified 5% CO₂ atmosphere) as indicated by the manufacturer.

2.5. MTT assay

The Cell Proliferation Kit I [3-(4,5-dimethylthiazol-2-yl)-2,5-diphenyltetrazolium bromide, MTT] Colorimetric assay (ROCHE, Basel, Switzerland) was used to evaluate the anti-proliferative effect of the extracts obtained from octopus' ink. The cells (1 × 10⁴ cells/well) were seeded in 96-well plates for 24 h. After medium removal, extracts were dissolved in DMSO and mixed with 10% fetal bovine serum-amended with Dulbecco's modified Eagle's medium (DMEM) (Gibco, Thermo Fisher Scientific, Waltham, MA, US), added (100 µL) to wells at several concentrations (25, 50, 100, 200 µg/mL), and incubated for 48 h at 37 °C. Before the last 24 h of incubation, 10 µL of MTT stock solution was added to each well, incubated for 4 h, and 100 µL sodium dodecyl sulfate (SDS) solution was added to each well. After 12 h incubation, plates were read at 570 nm, using a reference wavelength of 650 nm. The results were adjusted to a mathematical-biological model provided by NCSS statistical package (NCSS, NCSS LLC, East Kaysville, UT, US) and were expressed as half lethal concentration (LC₅₀) (µg/mL). These values were calculated for cancer cells, RAW 264.7, and ARPE-19 cells.

2.6. Fluorescence staining for DNA and cell membrane by DAPI and phalloidin

Structural and morphological changes in HCT116 cells, derived from the presence of DM-F2, were evaluated using the phalloidin and 4',6'-diamidino-2-phenylindole-tetramethylrhodamine B isothiocyanate (DAPI) dilactate staining (Van Vuuren, Botes, Jurgens, Joubert, & Van Den Bout, 2019). Briefly, HCT116 cells (1 × 10⁴ cells/well) were seeded in 96-well plates (24 h). After incubation, cells were treated with the DM-F2 extract (LC₅₀ = 52.64 µg/mL) for 48 h. Cells were then fixed with 3.7% formaldehyde in PBS and permeabilized with 0.2% Triton X-100 in PBS for 15 min. Afterward, cells were stained either with phalloidin (Sigma-Aldrich) or DAPI (Sigma-Aldrich) to visualize F-actin or the nuclear material through DNA, respectively. The microtitration plates were mounted and visualized on an inverted epifluorescence microscope (Leica DMi8, Leica Microsystems, Wetzlar, Germany).

2.7. Measurement of nitrites production

RAW 264.7 cells (2.5 × 10⁴ cells/well) were seeded in 96-well plates for 24 h. Then, the medium was removed, and the cells were treated with LPS (1 µg/mL) from *E. coli* O111:B4 (Sigma-Aldrich) and with the extracts (HX, EA, DM, WE, DM-F1, DM-F2, and DM-F3; 25–200 µg/mL) for 24 h. After 24 h-incubation, 100 µL of the cell supernatants were mixed with 100 µL of Griess reagent [0.1% N-(1-naphthyl)-ethylenediamine and 1% sulfanilamide in 5% H₃PO₄] and incubated in the dark (10 min; room temperature, RT: 25 ± 1 °C). The total production of nitrite was calculated based on the absorbance at 540 nm measured in the sample using a microtitration plate absorbance reader and contrasted to a standard curve of NaNO₂; results were expressed as half inhibitory concentration (IC₅₀, µg/mL) using LPS-induced RAW 264.7 cells as the positive control, and untreated cells as the negative control. The IC₅₀ values were calculated in the NCSS statistical software.

2.8. Measurement of intracellular reactive oxygen species (ROS) levels

Intracellular ROS levels were measured by the 2,7-dichlorodihydro-fluorescein diacetate (H₂DCFDA) assay. RAW 264.7 (2 × 10⁴ cells/well) were seeded in 96-well plates and incubated (24 h). After a medium replacement step, cells were incubated either with lipopolysaccharides (LPS) (1 µg/mL) dissolved either in DMEM or LPS + test fractions (HX, EA, DM, WE, DM-F1, DM-F2, and DM-F3; 25–200 µg/mL) for 22 h. The cells were then washed twice (PBS 100 µL, pH 7.4) and incubated with 5 µL of 20 µM 2',7'-dichlorodihydrofluorescein diacetate (H₂DCFDA, Thermo Fisher, Waltham, MA, US) in the darkness (30 min, RT). Fluorescence was measured at excitation/emission wavelengths of 485/530 nm in a fluorescence plate reader. The results were expressed in IC₅₀ (µg/mL).

2.9. Inflammatory cytokines array

The effect of DM-F2 on the modulation cytokines associated with inflammatory processes was assessed using the Mouse Cytokine Antibody Array Panel A (ARY0016, R&D Systems, Minneapolis, MN, US). RAW 264.7 cells (1 × 10⁶) were seeded in Petri dishes (60 mm) and allowed to grow and attach for 48 h. The cells were then treated either with LPS (1 µg/mL) or LPS + DM (IC₅₀ NO: 87.33 µg/mL) in fetal bovine serum (FBS)-free medium for 24 h (Luzardo-Ocampo et al., 2018). After the treatments, the cells were lysed (Halt™ Protease Inhibitor, Thermo Fisher Scientific, Waltham, MA, US) for 30 min at 4 °C, and protein concentration was measured by the bicinchoninic acid (BCA) assay (Pierce™ BCA Protein Assay, Thermo Fisher Scientific) to standardize all the treatments. The protein lysates were then assayed in the kit, following the manufacturer's instructions. The results were obtained using a ChemiDoc XRS + cell imaging system (BioRad Corp, Hercules, CA, US). The relative cytokine expression against the control was

visualized using the ImageQuant TL 8.1. software (General Electrics, GE Healthcare, Chicago, Illinois). The data were expressed as a fold change against the control (LPS-challenged RAW 264.7 cells). The protein network for bioinformatics analysis of the modulated cytokines was generated using the STRING® platform (von Mering et al., 2007) and edited in the Cytoscape® software. Data generated by the STRING analysis, including the enrichment Kyoto Encyclopedia of Genes and Genomes (KEGG) pathways and Enrichment Process, were normalized using the protein false discovery rate (FDR) values.

2.10. Analysis of IL-4 and NF-κB cell expression by flow cytometry

The impact of DM-F2 on the modulation of IL-4 and NF-κB was measured by flow cytometry using isolated mononuclear cells of human peripheral blood mononuclear cells (PBMCs) (Chávez-Sánchez et al., 2010). For this, PBMCs were isolated by a gradient of density using Ficoll-Paque PLUS (GE Healthcare), and the blood was diluted with PBS (1:2). Then, the top eluent was centrifuged (450 ×g, 30 min) with Ficoll-Paque, and the cells were then placed in a sterile test tube, washed with 100 µL of PBS, re-suspended in the culture medium, and counted. Before applying the treatments, the cells were examined before and after activation with LPS for 24 h. Then, the cells (1×10^6 cells/well) were treated either with LPS or DM-F2, and fluorescent markers for human IL-4 (Cat. 500806, BioLegend, San Diego, CA, US) and fluorescein isothiocyanate (FITC) anti-human IL-4 clone (MP4 25D2, BioLegend, San Diego, CA, US) were added. Nuclear factor-κB (NF-κB) was also evaluated after a 15 mM pre-treatment of cells with NF-κB antibody (Cat. B5681, Sigma-Aldrich) for 30 min. The fluorescence, expressed in relative fluorescence units (RFU), was measured in a BD FACSVerser™ flow cytometer (BD Biosciences, NY, US) after 10000 events analyzed.

2.11. In silico evaluation of interactions between DM metabolites and cytokines

The 3D structures of selected ligands for the *in silico* interaction were downloaded from PubChem database: 4-methylcaprolactam (PubChem CID: 19242), myristic acid (PubChem CID: 11005), hexadecanoic acid (PubChem CID: 985), hexadecanal (PubChem CID: 984), heptadecanal (PubChem CID: 71552), and octadecanal (PubChem CID: 12553). For the protein receptors, 3D structures of NF-κB (1LE5) and IL-2 (4YUE) were downloaded from the Protein databank. The other proteins (IL-1α, IL-1β, IL-3, IL-4, IL-7, IL-16, CCL17, and IL-27) were modeled in SwissModel based on their FASTA sequences from Uniprot® (P01582, P10749, Q5SX77, P07750, Q544C8, O54824, F6R5P4, and Q8K3I6, respectively). The best 3D structure based on their identity percentage was selected (Supplementary Table S1). The docking procedure conducted by Luna-Vital et al. (2017) was followed. The best binding sites were predicted in MetaPocket 2.0 online utility (Zhang et al., 2011), and the docking calculations were performed in AutoDock tools (Trott and Olson, 2010). The best docking conformation were plotted in Discovery Studio Visualizer v. 19.1.0.18287 software (Dassault Systèmes, Vélizy-Villacoublay, France).

2.12. Statistical analysis

Unless indicated, all data were expressed as the means ± SD of three independent experiments in triplicates. An analysis of variance (ANOVA) was conducted, followed by a *post-hoc* Tukey-Kramer's test ($p < 0.05$). All the analyses were carried out using the SPSS Statistics software.

3. Results

3.1. Anti-proliferative effect of *O. vulgaris* ink extracts and DM-fractions on cancer cells lines

Among the octopus ink extracts, DM exhibited the highest anti-proliferative activity on colorectal adenocarcinoma cell lines (HT-29 and HCT116) (Table 1) but did not show an inhibitory effect under 100 µg/mL in human breast adenocarcinoma cell line (MDA-MB-231). Since DM displayed the best biological effect on the HCT116 cell line, fractions were isolated (DM-F1, DM-F2, and DM-F3) and evaluated on the same cell line. None of the fractions were cytotoxic on the ARPE-19 cell line ($LC_{50} > 200$ µg/mL), but only the DM-F2 fraction exhibited a remarkable anti-proliferative effect, showing a lower ($p < 0.05$) LC_{50} than DM ($19.72 \pm 0.18\%$ lower). Both, cisplatin and docetaxel, were used as positive controls for anti-proliferative effect. Considering that the DM extract showed its highest anti-proliferative effect on HCT116 cells, its fractions were only assayed against this cell line.

3.2. Impact of DM-F2 extract on the morphological changes on HCT116 cells by DAPI and phalloidin staining

Compared to the negative control (untreated HCT116 cells), the 4 h exposition to DM-F2 induced morphological changes associated with cell death, such as the appearance of surface protrusions and membrane blebs, reduced pseudopods, and increased nuclear segmentation in HCT116 cells (Fig. 1).

3.3. Effect of *O. vulgaris* ink extracts on the cell viability, nitrites, and intracellular reactive oxygen species (ROS) inhibition on RAW 264.7 macrophages

RAW 264.7 cells were treated with several concentrations of the *O. vulgaris* extracts and DM soluble fractions for 24 h, and the cell viability was determined by the metabolic reduction of tetrazolium salt to a formazan dye (MTT assay) (Table 2). Except for EA, none of the extracts were cytotoxic ($LC_{50} > 100$ µg/mL). DM, DM-F2, and EA exhibited the lowest IC_{50} values for the inhibition of nitrites and ROS

Table 1

Anti-proliferative potential of *O. vulgaris* ink extracts, dichloromethane soluble fractions (DM-F1, DM-F2, and DM-F3), and drug controls on human cell lines at 48 h of incubation.

Extracts	Non-cancerous cell (LC_{50} , µg/ml)	Cancerous cells (LC_{50} , µg/ml)		
		ARPE-19	HCT116	MDA-MB-231
HX	>200 ^{Aa}	>200 ^{Aa}	>200 ^{Aa}	>200 ^{Aa}
EA	>200 ^{Aa}	75.7 ± 4.8 ^{Cb}	143.6 ± 4.6 ^{Bb}	85.6 ± 3.5 ^{Cc}
DM	192.7 ± 20.8 ^{Aa}	65.6 ± 3.9 ^{Db}	108.6 ± 5.1 ^{Bc}	81.6 ± 5.0 ^{Cc}
WE	>200 ^{Aa}	>200 ^{Aa}	>200 ^{Aa}	>200 ^{Aa}
DM-F1	>100 ^{Bd}	>200 ^{Aa}	–	–
DM-F2	>100 ^{Ad}	52.6 ± 3.0 ^{Bc}	–	–
DM-F3	>100 ^{Bd}	>200 ^{Aa}	–	–
Cisplatin	137.9 ± 6.5 ^{Bb}	7.4 ± 0.7 ^{De}	152.1 ± 4.7 ^{Ab}	103.9 ± 0.6 ^{Cb}
Docetaxel	110.3 ± 4.5 ^{Ac}	11.0 ± 2.5 ^{Bd}	9.0 ± 1.3 ^{Bd}	2.4 ± 0.0 ^{Cd}

The values are expressed as the means ± from three different experiments in triplicates. Different lower-case letters by columns indicate significant differences ($p < 0.05$) between treatments, for each cell line, by Tukey-Kramer's test. Different upper-case letters by row are significantly different ($p < 0.05$), between cell lines and for each treatment, by Tukey-Kramer's test. DM: Dichloromethane extract; DM-F1, F2, F3: Purified fractions from the DM extract; EA: Ethyl acetate extract; HX: Hexane extract; WE: Water extract.

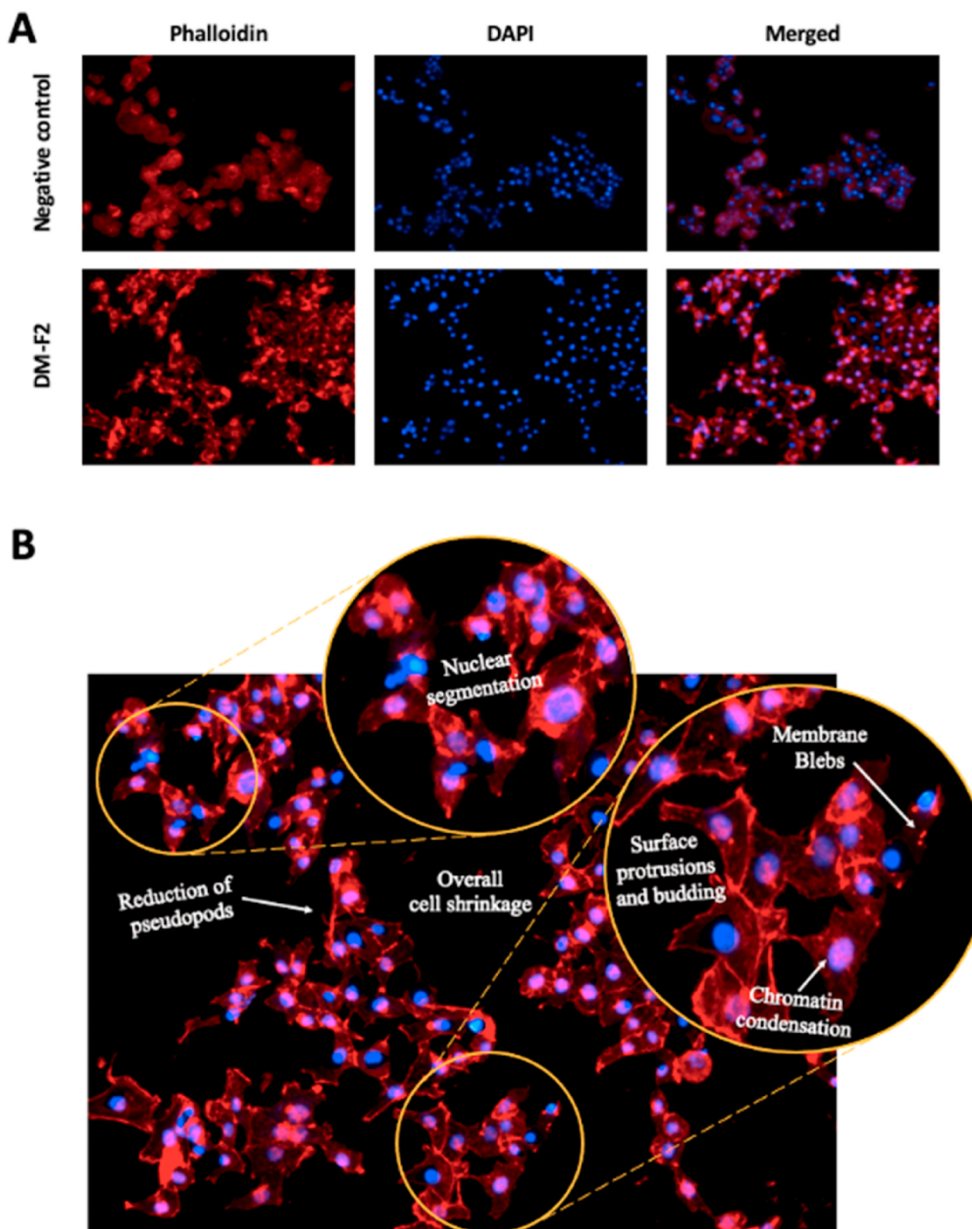


Fig. 1. (A) Effect of DM-F2 on the morphology of HCT116 cells after staining with DAPI and phalloidin; (B) Morphological changes associated to apoptotic cell death. DAPI: 4'-6-diamidino-2-phenylindole dilactate; DM-F2: Fraction 2 from dichloromethane extract (DM) of *O. vulgaris* ink.

production. DM-F1, DM-F2, HX, and WE did not show inhibitory potential against the same parameters. Outstandingly, DM-F2 IC₅₀ values for inhibiting nitrites and ROS production were significantly ($p < 0.05$) lower than DM (51.72 ± 1.07 and $23.67 \pm 6.22\%$ lower, respectively). Since DM-F2 was not cytotoxic, reductions of NO and ROS are linked to anti-inflammatory mechanisms rather than reductions in cell viability.

3.4. Untargeted metabolomic analysis of volatile compounds from DM and DM-F2

For the untargeted metabolomic analysis of the most biologically active components of the extracts (DM and DM-F2) (Fig. 2), the generated heatmap (Fig. 2A) clustered the samples into two different groups, being hexadecanoic acid, myristic acid, and 1-tetradecanol, the most abundant compounds in the DM extract. At the same time, octadecanol, 1-(15-methyl-1-oxohexadecyl) pyrrolidine, and 9-octadecenamide were the most abundant compounds in the DM-F2 extract.

The predicted involvement of these compounds in selected metabolic

pathways from the KEGG database (Fig. 2B) showed that most of them are related to very-long-chain fatty acids, fatty acids biosynthesis, plasmalogen synthesis, and elongation in mitochondria pathways. The analysis of variable in importance (VIP) scores for all the identified compounds by GC-MS (Fig. 2C) from DM (A) and DM-F2 (B) highlighted octadecanol, hexadecanoic acid, myristic acid, and 1-(15-methyl-1-oxohexadecyl) pyrrolidine as the compounds with the highest VIP values (~1.4–1.8). Enrichment analysis of the compounds for the predictive involvement in potential metabolic pathways associated them with fatty acids pathways such as the biosynthesis of unsaturated fatty acids, N-glycan biosynthesis, fatty acid degradation, and fatty acid elongation (Fig. 2D). The metabolomic analysis was conducted based on the identified metabolites from DM (Supplementary Table S1) and DM-F2 (Supplementary Table S2).

Table 2

Effect of *O. vulgaris* ink extracts and dichloromethane soluble fractions on the production of nitrites, reactive oxygen species production (ROS), and cell viability of RAW 264.7 cells.

Extracts	RAW 264.7 ($\mu\text{g}/\text{ml}$)		
	IC ₅₀ Nitrites	IC ₅₀ ROS	LC ₅₀ Cell viability
HX	195.0 \pm 5.8 ^a	>200 ^a	>200 ^a
EA	47.8 \pm 4.7 ^d	52.8 \pm 4.7 ^d	67.7 \pm 4.7 ^c
DM	61.9 \pm 4.5 ^c	87.3 \pm 1.9 ^c	100.9 \pm 4.4 ^b
WE	>200 ^a	>200 ^a	>200 ^a
DM-F1	>200 ^b	>200 ^b	>200 ^b
DM-F2	29.9 \pm 2.8 ^e	66.7 \pm 6.9 ^d	>200 ^b
DM-F3	>200 ^b	>200 ^b	>200 ^b

The values are expressed as the means \pm from three different experiments in triplicates. Different letters within columns indicate significant differences ($p < 0.05$) by Tukey-Kramer's test. Cells were exposed to 24 h-treatment. DM: Dichloromethane extract; DM-F1, DM-F2, DM-F3: DM fractions; EA: Ethyl acetate extract; HX: Hexane extract; ROS: Intracellular reactive oxygen species; WE: Water extract.

3.5. Effect of DM-F2 on the modulation of cytokines produced by RAW 264.7

Out of 40 cytokines, 8 were differentially up-regulated (>1.5 fold) (CCL17, IL-16, IL-7, IL-4, IL-3, IL-1 β , IL-1 α , and G-CSF) (Fig. 3A). The functional relationship of these cytokines based on fusion evidence, neighborhood evidence, and the existing databases after the bioinformatics analysis (STRING®) (Fig. 3B) indicated that most cytokines are involved in the cytokine-cytokine receptor interaction, inflammatory bowel disease (IBD), the Janus kinase signal transducer and activator of transcription (JAK-STAT) pathway, maturation and differentiation of immune cells, IL-17, and the phosphatidylinositol-3-kinase (PI3K/Akt) pathway (Fig. 3C). As a result of this involvement, the modulated cytokines suggested the capability of octopus ink to target the regulation of signaling receptor activity, response to a stimulus, the immune response, and cytokine production (Fig. 3D). Outstandingly, the DM-F2 extract increased the expression of the anti-inflammatory cytokine IL-4 and decreased the expression of the nuclear factor- κ B (%) on PBMCs (52.61 \pm 0.10% and $-54.47 \pm 2.75\%$, respectively) (Fig. 3E).

3.6. In silico interactions of DM compounds and cytokines

Conventional hydrogen bond and pi-alkyl bonding interactions were shared among all the interactions, but the highest affinity was found for IL-1 α (Fig. 4A) (-5.6 kcal/mol, Table S1), while the lowest was IL-1 β (Fig. 4B) (-4.1 kcal/mol, Table S1).

Unlike the interactions shown in Fig. 4, a higher diversity of bonding interactions was found between the selected proteins such as pi-sigma (Fig. 5A) and carbon-hydrogen bond (Fig. 5B), but alkyl and pi-alkyl were common among the three depicted interactions. As shown in Table S1, interactions with IL-1 α were those with the highest binding affinity (-5.8 kcal/mol) and IL-2 the lowest (-4.6 kcal/mol).

The affinity interactions from hexadecanoic acid and 1-(15-methyl-oxohexadecyl) were selected since they exhibited the highest binding affinity energy (Table S1) among all the assayed compounds, which were considered from the VIP scores analysis (Fig. 2C).

4. Discussion

It has been well established that pro-inflammatory factors could trigger the development of cancer-associated conditions (Lichtenstern et al., 2020). Consequently, natural anti-inflammatory compounds might deliver an appropriate anti-cancer response without the observed adverse effects produced by traditional chemical compounds used in the cancer treatment (Taylor et al., 2019). As a potential source of anti-inflammatory compounds with selective anti-proliferative effect,

biologically active molecules from *O. vulgaris* ink might valorize this underutilized natural product, scarcely used in certain food preparations around the world. Despite this potential, most research is focused on cuttlefish ink, and exploration of the health-derived benefit from octopus is still underdeveloped (Derby, 2014), yet some works have focused on octopus' antimicrobial peptides. For example, some researchers have reported the antimicrobial potential of peptides from the posterior salivary glands of *O. vulgaris* (Almeida et al., 2020). The authors informed about several peptide sequences identified by LC-MS/MS, most of them from known venom families such as serine proteases, metalloproteases, and serine proteases inhibitors, that were associated *in silico* with systemic anti-inflammatory responses and antimicrobial effects. Moreover, an *O. vulgaris*' suckers aqueous extract (1 mg/mL) showed inhibition of *Staphylococcus aureus*, *Pseudomonas aeruginosa*, and *Candida albicans* (80% minimal inhibitory concentration, MIC₈₀: 50–150 μM for 4 identified peptidic sequences) effect associated with peptides identified by nano liquid chromatography coupled to quantitative electrospray ionization and mass spectrometry analysis (LC-ESI-Q-Orbitrap MS/MS) (Maselli et al., 2020). The observed antibacterial activity is not only associated with *O. vulgaris* components but also to hemocytes (hemoblast-like cells, hyalinocytes, and granulocytes) carrying out demonstrated antibacterial activity mainly against *S. aureus*, *Listeria monocytogenes*, *Bacillus cereus*, *Salmonella* spp., and *P. aeruginosa* (bactericidal activity: ~60–90%) (Troncone et al., 2015).

Regarding other cephalopods species, Zhong et al. (2009) assessed the antioxidant potential of *Sepia officinalis* ink *in vivo* using Balb/c mice, finding a significant ($p < 0.05$) reduction of antioxidant enzymes' activities such as catalase, glutathione peroxidase, superoxide dismutase, and malonaldehyde. The authors attributed this effect to the synergistic effects of some ink's components such as melanin, proteins, lipids, and glycosaminoglycans. In another study, Girija et al. (2012) reported the antibacterial activity of the hexane extract from Indian squid (*Loligo duvaucelii*) ink on *Escherichia coli* and *Klebsiella pneumoniae* bacterial strains. The same authors also reported a novel protein isolated from the melanin-free ink fraction (Lolduvin-S), also exhibiting inhibitory effects against gram-positive bacterial and pathogenic yeasts Girija et al. (2011).

The standardization of the ink-obtaining procedure from marine products is crucial to extract high quality ink without affecting the ink's chemical composition. For instance, it has been reported that depending on the collection method, specific components such as L-3,4-dihydroxyphenyl-alanine can be found, while epinephrine or selected proteins could be damaged (Madaras et al., 2010). Therefore, in this research, a standardized procedure was followed to obtain ink extracts using several solvents based on chemical affinity to extract selected compounds. These extracts were initially screened for their anti-proliferative potential on representative cancer cell lines from highly deadly cancer conditions (Bray et al., 2018). Despite the absence of reports depicting the anti-proliferative potential of *O. vulgaris* ink, several reports can be found underlining the anti-proliferative activity from cuttlefish ink. Soufi-Kechaou et al. (2017) reported the antitumoral activity of isolated and purified peptides from *O. vulgaris* and *Sepia officinalis* ink, observing a higher ($p < 0.05$) decrease of IGR 39 (melanoma cells) adhesion from *O. vulgaris*-derived peptides. However, peptides (10–30 mg/mL) from *S. officinalis* caused a higher inhibition of cell migration than that observed when counterparts from *O. vulgaris* were used, suggesting major anti-metastatic dissemination. More recently, our research group underlined the anti-proliferative potential of *O. vulgaris* ink fractions, where the same DM fraction showed the highest inhibitory effects against 22Rv1 prostate carcinoma cells (LC₅₀: 68.2 $\mu\text{g}/\text{mL}$) (Hernández-Zazueta et al., 2021). The obtention of several DM fractions indicated that DM-F2 was the most biologically active, inducing 22Rv1 apoptosis (transition to late and early apoptosis) and increasing intracellular reactive oxygen species (ROS) production compared to the untreated cells.

For other cephalopods, it has been reported that *Sepia esculenta* ink

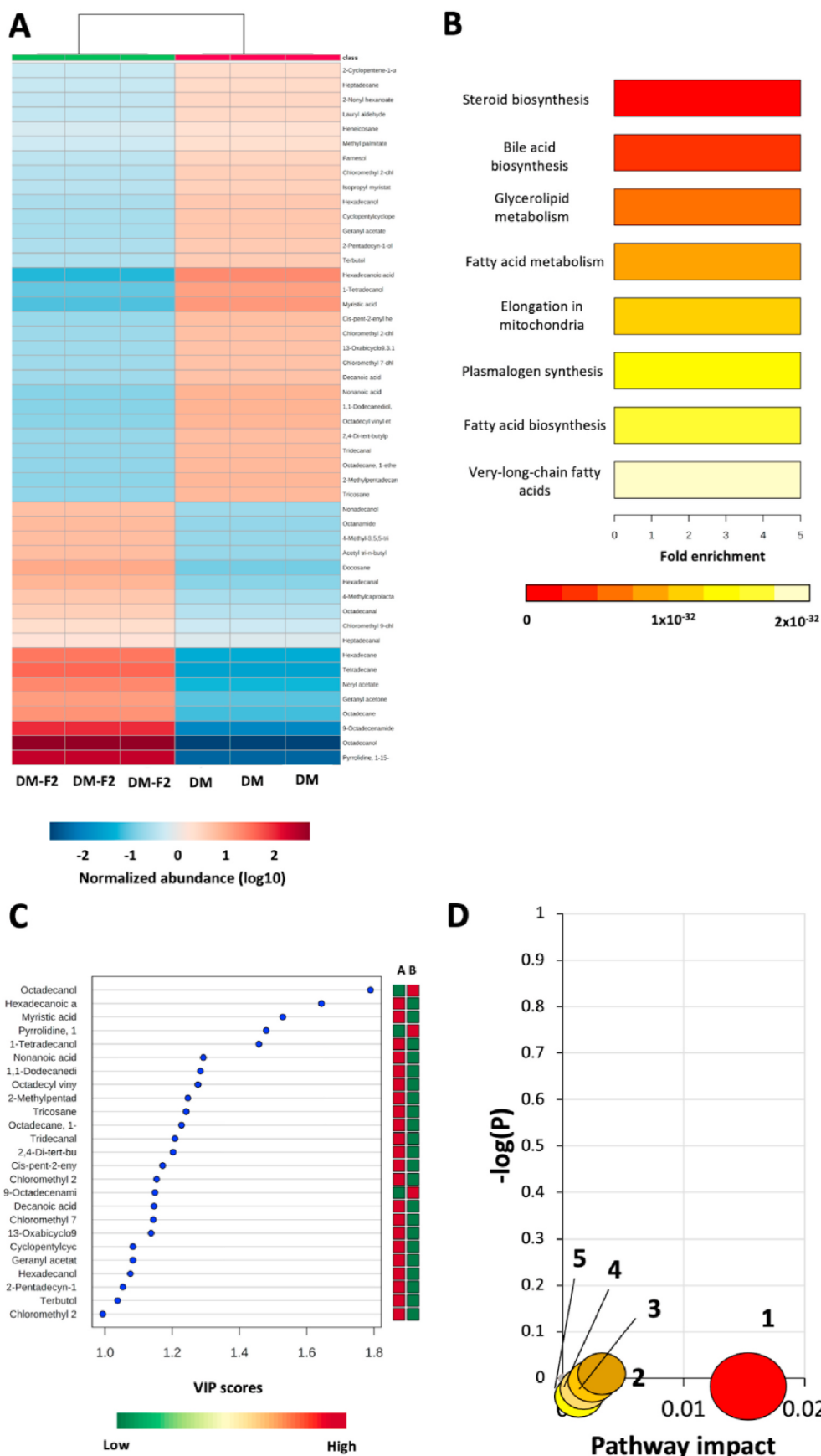


Fig. 2. Untargeted metabolomic analysis of DM and DM-F2 extracts. (A) Heatmap clustering for the identified volatile compounds from DM and DM-F2; (B) Enrichment pathways analysis; (C) VIP scores from the partial least squares (PLS) analysis; (D) Pathways impact from the metabolomic arrangement of compounds.

For Fig. 2C, A: DM and B: DM-F2. For Figs. 2D and 1: Fatty acid biosynthesis; 2: fatty acid elongation; 3: fatty acid degradation; 4: N-glycan biosynthesis; 5: biosynthesis of unsaturated fatty acids.

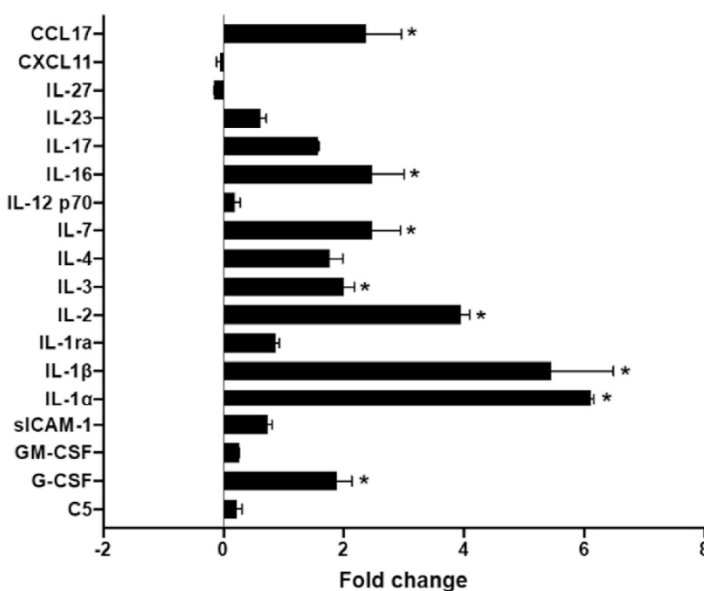
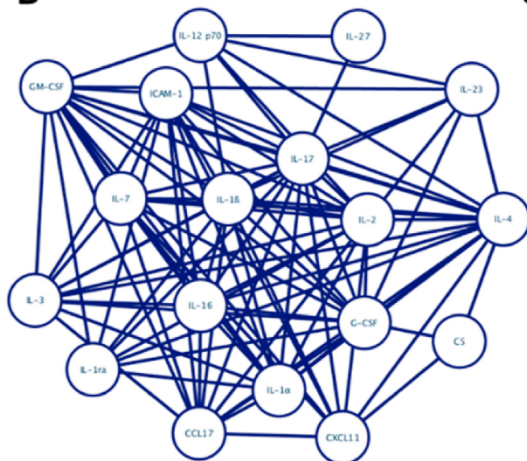
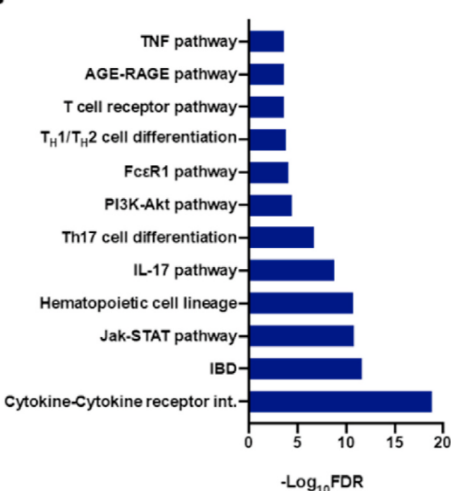
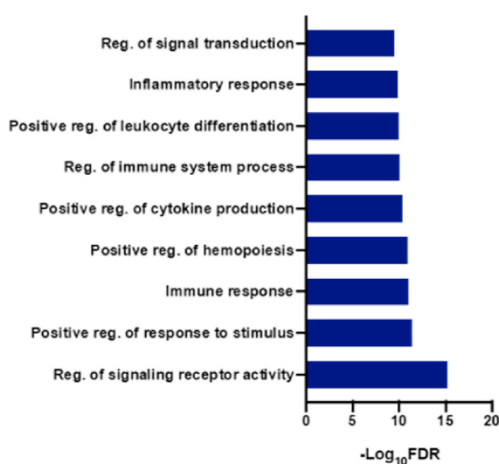
A**B****C****D**

Fig. 3. Expression and association of cytokines involved in the inflammatory process mediated by the DM-F2 on LPS-stimulated RAW 264.7 macrophages and PBMCs. (A) Effect of DM-F2 on cytokine expression; (B) Functional associations of cytokines; (C) KEGG pathways associated with the differentially expressed cytokines; (D) Biological processes related to the modulation of the cytokines; (E) Regulation of anti-inflammatory (IL-4) and pro-inflammatory cytokines (NF-κB) analyzed by flow cytometry on PBMCs cells.

The cytokines data (Fig. 3A) are expressed as fold change relative to the negative control (LPS-stimulated RAW 264.7) and corresponded to the average of two independent experiments. Asterisks (*) corresponded to significant fold-change. Lines in the cytokines network (Fig. 3B) represent the proteins cytokines interaction. Values from flow cytometry analysis are the means \pm SD of three independent experiments in triplicates (Fig. 3E). Different letters indicate significant differences ($p < 0.05$) by Tukey-Kramer's least significant difference test. The negative control corresponded to untreated PBMCs, while the positive control is LPS-stimulated PBMCs cells (LPS: 1 μ g/mL). AGE-RAGE: Advanced glycation end-products-Receptor for AGE; DM-F2: Fraction 2 from dichloromethane extract; FDR: False discovery rate; T_H: T-helper cells; FcεR1: FCε receptor 1; sICAM-1: Soluble forms of intercellular adhesion molecule 1; GM-CSF: Granulocyte-macrophage colony-stimulator factor; G-CSF: Granulocyte colony-stimulator factor; JAK-STAT: Janus kinase-signal transducer and activator of transcription; IBD: Inflammatory bowel disease; PI3K-Akt: Phosphatidylinositol-3-kinase.

E

	IL-4		NFκB
Control (-)	421.66 \pm 6.66 ^b		160.33 \pm 47.77 ^b
Control (+)	287.00 \pm 3.46 ^c		192.33 \pm 12.86 ^a
DM-F2	438.00 \pm 5.57 ^a		87.33 \pm 0.58 ^c

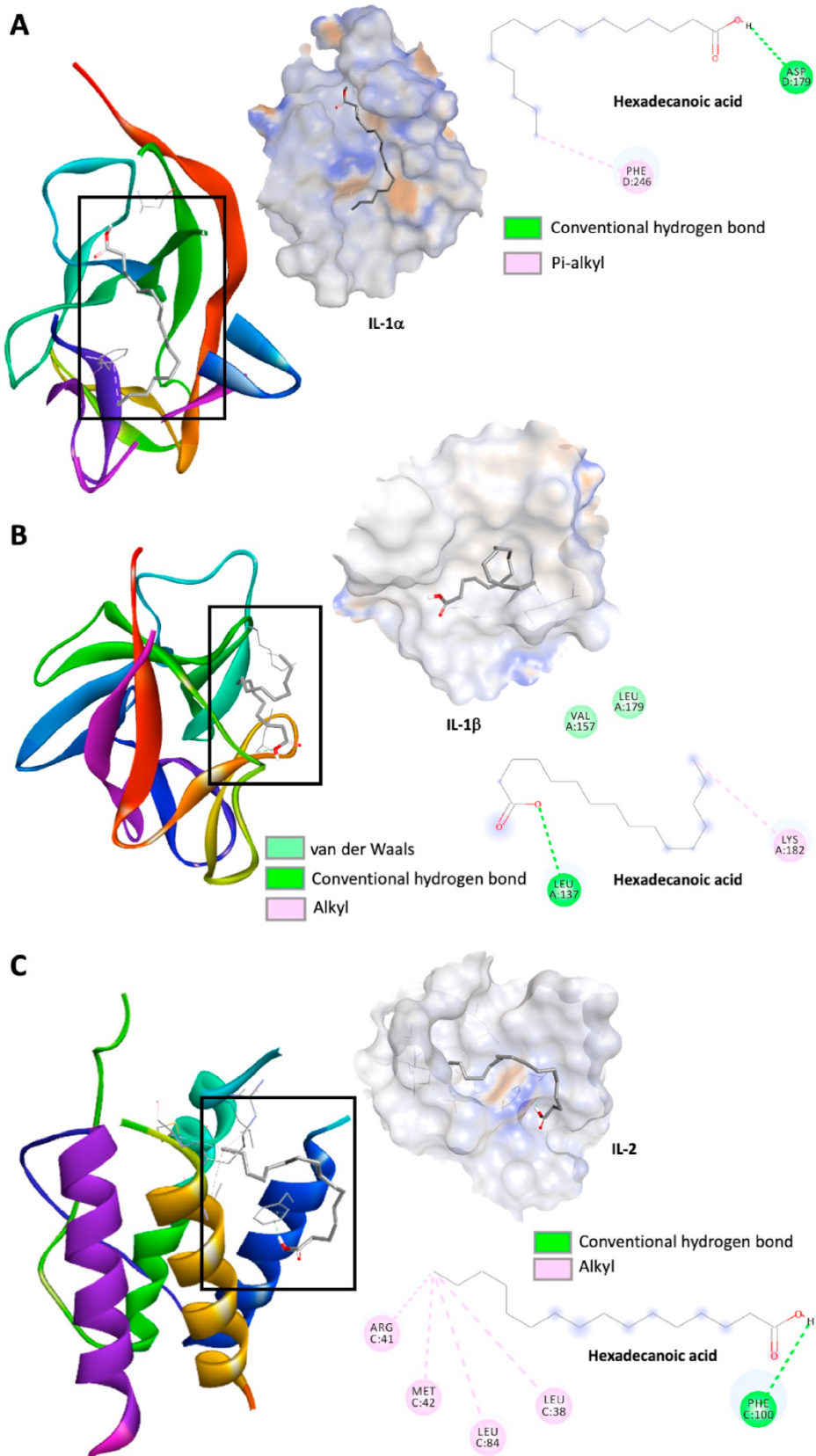


Fig. 4. Best *in silico* interactions between hexadecanoic acid and selected proteins modulated by DM extract: (A) IL-1 α , (B) IL-1 β , and (C) IL-2. The results show the best docking poses between each selected protein and hexadecanoic acid as indicated by AutoDock Vina. Images were generated with BioVia Discovery software.

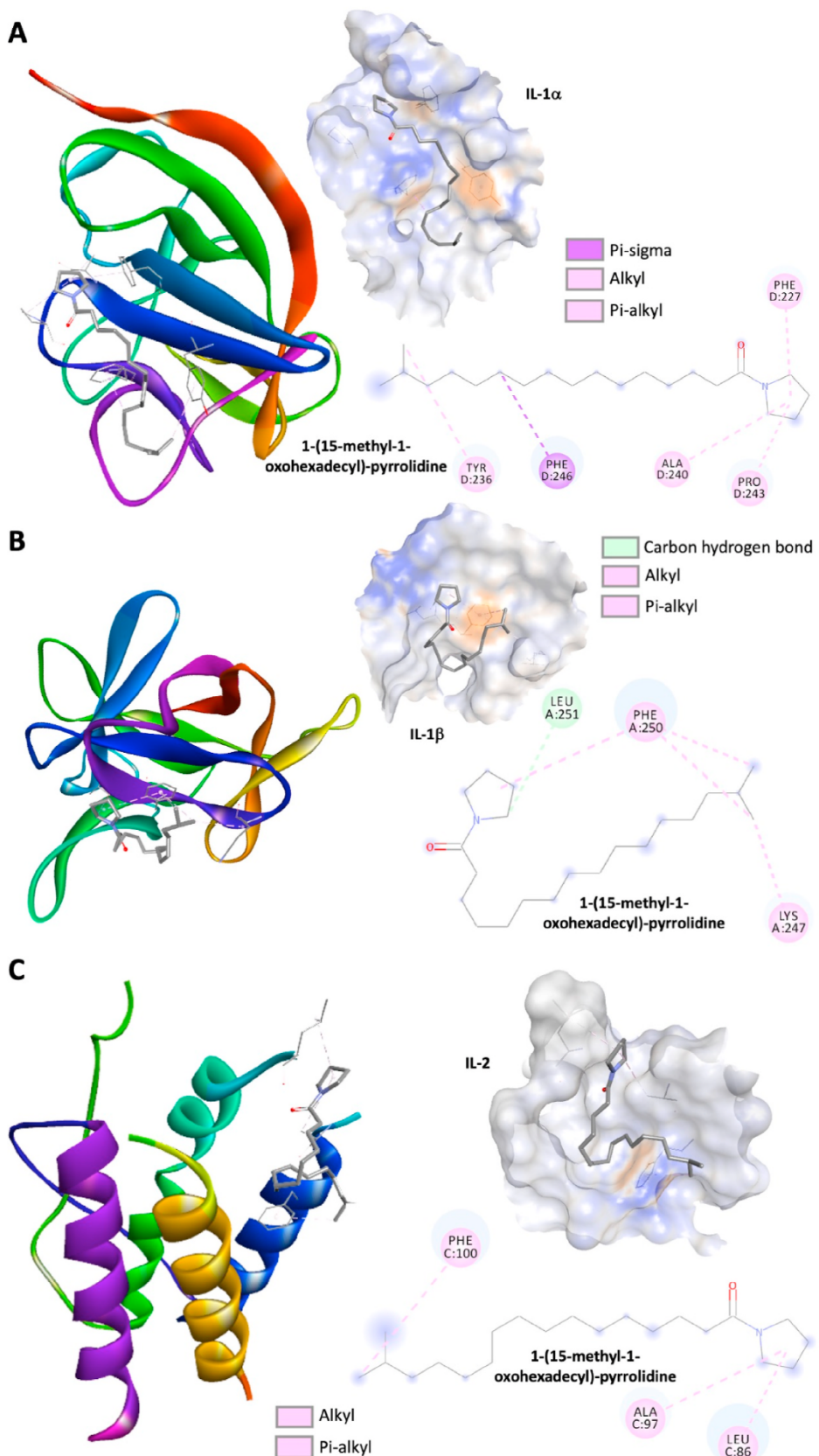


Fig. 5. Best *in silico* interactions between 1-(15-methyl-1-oxohexadecyl)-pyrrolidine and selected proteins modulated by DM extract: (A) IL-1 α , (B) IL-1 β , and (C) IL-2.

The results show the best docking poses between each selected protein and hexadecanoic acid, as indicated by AutoDock Vina. Images were generated with BioVia Discovery software.

exhibits antitumor activity *in vivo* against Meth-A fibrosarcoma from BALB/c mice, and its peptidoglycan-containing fraction also showed this activity (Guo-fang et al., 2011). Russo et al. (2003) reported an LC₅₀ of 81 µg/mL in Caco-2 colorectal adenocarcinoma cells from the melanin-free ink extract of *Sepia officinalis*, attributed to its tyrosinase activity-inducing oxidative damage to DNA, lipids, or proteins, inactivating vital cell functions and promoting caspase-3 mediated apoptosis.

The anti-proliferative effect of cisplatin relies on its capability to enhance the TNF-related apoptosis-inducing ligand (TRAIL). However, it has shown limited effect against A549 and MDA-MB-231 cancer cell lines due to TRAIL synchronization with other signaling complexes or the need for specific death receptors (DR4 and DR5) to transmit the pro-apoptotic signal (Gasparian et al., 2017). Docetaxel has demonstrated the capability of disrupting the microtubule network that blocks cell cycles in the late G2 and M phases and it has been mainly used to treat breast and prostate cancer (Sohail et al., 2018).

The further examination by DAPI and Phalloidin staining of the DM-F2 effects on HCT116 confirmed its enhanced capability to cause apoptosis-inducing modifications such as chromatin fragmentation (pyknosis) and cytoskeleton breakdown. (Coleman et al., 2001; Yuan et al., 2007). No reports of *in vitro* structural changes induced by *O. vulgaris* ink extracts were found, but oligopeptides isolated from *Sepia esculenta* ink have been observed to cause a significant increase in the fluorescence of human A549 lung cancer cells, as examined by DAPI-/FITC staining (Zhang et al., 2017). These effects were in line with the inhibition of proliferation and apoptosis induction in the same cell line.

The production of nitrites has been classically linked to an indirect measurement of nitric oxide production, a key mediator of the pro-inflammatory response, and a mediator of the redox modification of protein and other biomolecules (Freeman et al., 2017). The high reactivity of NO molecule with oxygen, superoxide, and hydrogen peroxide, target the intracellular production of ROS, contributing to inflammation and potentially pro-carcinogenic cell damage (DNA damage and mutations) (Brüne et al., 2003; Lonkar and Dedon, 2011). There are no reports on the NO and ROS modulation by *O. vulgaris* ink, but few studies have reported promising effects from squid ink. For instance, polysaccharides isolated from *Sepia esculenta* ink inhibited ROS production (~55%) in H₂O₂-treated human dermal fibroblasts (HDFs) (200 µM) and regulated HDFs oxidative stress by reducing malonaldehyde (MDA), superoxide dismutase (SOD), and glutathione peroxidase activity, compared to a H₂O₂ control (Chen et al., 2020). Another polysaccharide extract from *S. esculenta* decreased plasmatic ROS, SOD, and MDA levels from cyclophosphamide-treated male Kunming mice (6 weeks age) (Gu et al., 2017).

Fatty acids (FA) are a major class of compounds found in the ink of marine animals such as squids, cuttlefish, and octopus. Thus, the metabolomic analysis naturally associated most DM and DM-F2 compounds with FA biosynthesis (Fig. 2B) (Derby, 2014). Hence, the results obtained from Fig. 2C classified several FA as metabolites, fitting within the partial-least-squares model, allowing the discrimination of other metabolites with VIP ≥2 (Herrera-Cazares et al., 2019; Luzardo-Ocampo et al., 2020). Among the involved pathways, fatty acid biosynthesis reached the most significant impact, while the other pathways were classified with the same impact (Fig. 2D).

The potential anti-inflammatory and anti-proliferative activity of some of these fatty acids has been reported (Santos et al., 2013; Wang et al., 2009). Hexadecanoic or palmitic acid has been previously identified as one of the most abundant saturated fatty acids from crustaceans, such as caramote prawn (*Penaeus kerathurus*) and mantis shrimp (*Squilla mantis*), reaching up to 50–60% (Balzano et al., 2017). Besides, these fatty acids have been found in erythrocytes from fish consumers, partially linked to a lower risk of breast cancer (Kuriki et al., 2007). Octadecanol is a volatile oil that has been identified as a potential metabolite associated with reduced local inflammation in LPS-challenged isolated mouse peritoneal macrophages, showing a decrease in the nitrites production, TNF-α, and inducible nitric oxide

synthase (iNOS) (Li et al., 2013).

There are no reports about the biological activity of 1-(15-methyl-1-oxohexadecyl) pyrrolidine. 9-octadecenamide is an oleamide that has been identified in *Sepia pharaonis* ink extracts and biologically acts as a bioactive lipid signaling molecule in several organisms. (Ebenezer et al., 2020). Moreover, a potent anti-inflammatory activity *in vitro* in the LPS-activated BV2 murine microglial cell line has been reported for 9-octadecenamide, decreasing nitrite concentrations and PGE₂ production by blocking iNOS and COX-2 expression, both converging in inhibiting NF-κB DNA binding and transcription (Oh et al., 2010).

Due to their modulation of pro-inflammatory pathways, bioactive compounds from natural food sources have shown promising effects as cancer treatment coadjutants. The JAK-STAT is an essential cellular regulatory pathway that involves multiple proteins, whereas its regulation offers a valuable opportunity to disrupt cell proliferation, modulate the transduction of extracellular signals, and control inflammation (Groner and von Manstein, 2017). As observed by the cytokine regulation, most bioactive compounds of the ink act as signal transducer regulators, serving as a bridge in the interplay between the inflammation development and the maturation of immune cells. The JAK-STAT pathway is critical in lymphocyte development, influencing their fate into differentiation to naive T cells or inflammatory T cell lineages (Egwuagu, 2009). These processes align with the effect of squid ink on increased TNF-α levels in NK-cells *in vivo*, suggesting an immuno-stimulatory activity on NK cells and macrophages to inhibit tumor cells (Changlong et al., 1999). Another immuno-regulatory activity from this pathway converges in the production of IL-17 by Th17 cells, acting in the host defense against bacteria and fungi (Ma et al., 2012). Thus, the potential of the ink components to contribute to the host defense against pathogens can also be suggested.

Joint anti-inflammatory and anti-cancer effects from the ink of marine animals also comprise the regulation of the PI3K-Akt and the mitogen-activated protein kinase (MAPK) pathway, which are common in multiple stages of carcinogenesis because both participate in a p53-dependent pathway (Pencik et al., 2016). Polysaccharides from *Sepia esculenta* ink, mainly composed of monosaccharides, galactosamine, and arabinose, have exhibited *in vivo* protection against cyclophosphamide-induced cytotoxicity through PI3K/Akt and p38 MAPK-induced apoptosis and autophagy (Liu, Tao, et al., 2016). On MDA-MB-231 cells, the same polysaccharide extract showed tumor metastasis inhibition, downregulating MMP-2 and MMP-9 metalloproteases and inhibiting key pro-angiogenic pathways for the cancer survival and spreading (Liu, Xiao, et al., 2016). In another study, *Sepia esculenta* ink polysaccharides induced *in vivo* the expression of IL-6, IL-10, and TNF-α on epithelial cells (Zuo et al., 2014). Since these polysaccharides also induced the expression of the immunoglobulin A gene (IgA J chain gene), IgA contents in the intestinal tracts of the exposed mice were elevated (Lu et al., 2016). The authors hypothesized that ink polysaccharides mediate among gut microbiota and metabolites, the intestinal epithelial cells, brain-gut axis circuit, and the host metabolism. Consequently, the capability of *O. vulgaris* ink's components to regulate both inflammation and cancer might be involved in the production of the basal level of cytokines to effectively respond to the immune development and the recognition of cancer cells to undergo apoptosis. Since the ink components are also up-regulating the production of IL-1, IL-2, and IL-4, it could be inferred a potential immunomodulatory activity on potential tumor development or the blockade of the cancer maintenance (Setterrrahmane and Xu, 2017).

Overall, all of the assayed compounds displayed low binding energies, suggesting that other metabolites might be involved in the observed beneficial effects from *O. vulgaris* ink extracts. These compounds were selected based on those with the highest overall VIP score for both DM and DM-F2 composition, but only those with the lowest binding energies [hexadecanoic acid and 1-(15-methyl-1-oxohexadecyl) pyrrolidine] (Supplementary Table S1) were chosen for the graphics. As the highest affinity was found for IL-1α, it could be inferred a significant

influence of the anti-inflammatory and anti-proliferative compounds on related pathways, which are involved by the controlled activity between selected receptors, the participation of exogenous agents that mediate in the activation of caspase-1 and the inflammasome-derived production of IL-1 β (Gabay et al., 2010). Findings indicating cholesterol crystals' capability to activate the NLRP3 inflammasome in macrophages, inducing lysosomal destabilization by the leakage of cathepsin B into the cytoplasm could also confirm this hypothesis (Rajamäki et al., 2010). Nonetheless, as an anti-inflammatory activity was observed from the reduction of the production of nitrites and intracellular ROS, it could be inferred that this pro-inflammasome activity might be acting at the basal level or this overactivation should not be considered pro-inflammatory stimuli, highlighting the not fully understood dual roles of the inflammasome activation (Kelley et al., 2019).

A summary of the observed anti-inflammatory effects is indicated in Fig. 6. The black arrows indicate the influence of DM extract in the production of each cytokine. Bioactive compounds from DM-F2 were involved in several pathways. Increments in the production of IL-2, IL-4, IL-27, and IL-23 were associated with overactivation of the JAK-STAT pathway, while the extract inhibited the assemblage of the NF- κ B protein complex by inhibiting the IL-17 associated pathway. Since IL-1 α results from the inflammasome activation, requiring the first stimulus due to NF- κ B, increments in its production might be at basal levels since there are no other stimuli that could initiate its activation, such as calcium or ROS production. Several cytokines involved in the LPS-stimulated TLR4 activation were produced, such as G-CSF, GM-CSF, CXCL11, and IL-12, indicating the capability of the DM-F2 bioactive compounds to collaborate in coordinated recruitment of immune cells to the inflammation sites to locally exert a pro-inflammatory effect at basal levels, as demonstrated by nitric oxide and NF- κ B reductions.

The results from this research suggested the potential immunomodulatory and anti-proliferative dual roles of *O. vulgaris* ink components. *O. vulgaris* ink extracts exerted anti-proliferative effects on two colorectal (HCT116 and HT-29) and breast (MDA-MB-231) cancer cell lines. A purified dichloromethane fraction (DM-F2) from the ink exhibited the highest biological activity contributing to the induction of apoptotic-like morphological changes on HCT116 cells. Besides, this

fraction exerted an anti-inflammatory effect on LPS-stimulated RAW 264.7 cells reducing the production of nitrites, ROS, and up-regulating cytokines involved in the JAK-STAT, MAPK, PI3K-Akt, and the canonical NF- κ B pathway. The metabolomic analysis suggested that fatty acids and aldehydes from the DM-F2 could be responsible for these effects, potentially binding with inflammation/cancer targets such as IL-1 α , IL-1 β , and IL-2. This evidence underlines the beneficial anti-inflammatory and anti-proliferative effects of bioactive compounds from underutilized natural food products such as *O. vulgaris* ink.

CRediT authorship contribution statement

Martín S. Hernández-Zazueta: Formal analysis, Data curation, Writing – original draft, Conceived and designed the analysis, Collected the data, Contributed data or analysis tools, Performed the analysis, Wrote the paper. **Iván Lizardo-Ocampo:** Formal analysis, Data curation, Writing – original draft, Conceived and designed the analysis, Collected the data, Contributed data or analysis tools, Wrote the paper. **Joel S. García-Romo:** Formal analysis, Data curation, Writing – original draft, Contributed data or analysis tools, Performed the analysis. **Luis Noguera-Artiaga:** Formal analysis, Data curation, Writing – original draft, Contributed data or analysis tools, Performed the analysis, Wrote the paper. **Ángel A. Carbonell-Barrachina:** Formal analysis, Data curation, Writing – original draft, Conceived and designed the analysis, Performed the analysis, Wrote the paper. **Pablo Taboada-Antelo:** Formal analysis, Data curation, Conceived and designed the analysis, Contributed data or analysis tools. **Rocío Campos-Vega:** Formal analysis, Data curation, Conceived and designed the analysis, Contributed data or analysis tools. **Ema Carina Rosas-Burgos:** Formal analysis, Data curation, Conceived and designed the analysis, Contributed data or analysis tools. **María G. Burboa-Zazueta:** Formal analysis, Data curation, Conceived and designed the analysis, Contributed data or analysis tools. **Josafat M. Ezquerro-Brauer:** Formal analysis, Data curation, Conceived and designed the analysis, Other contribution. **Armando Burgos-Hernández:** Formal analysis, Data curation, Writing – original draft, Conceived and designed the analysis, Collected the data, Contributed data or analysis tools, Performed the analysis, Wrote the

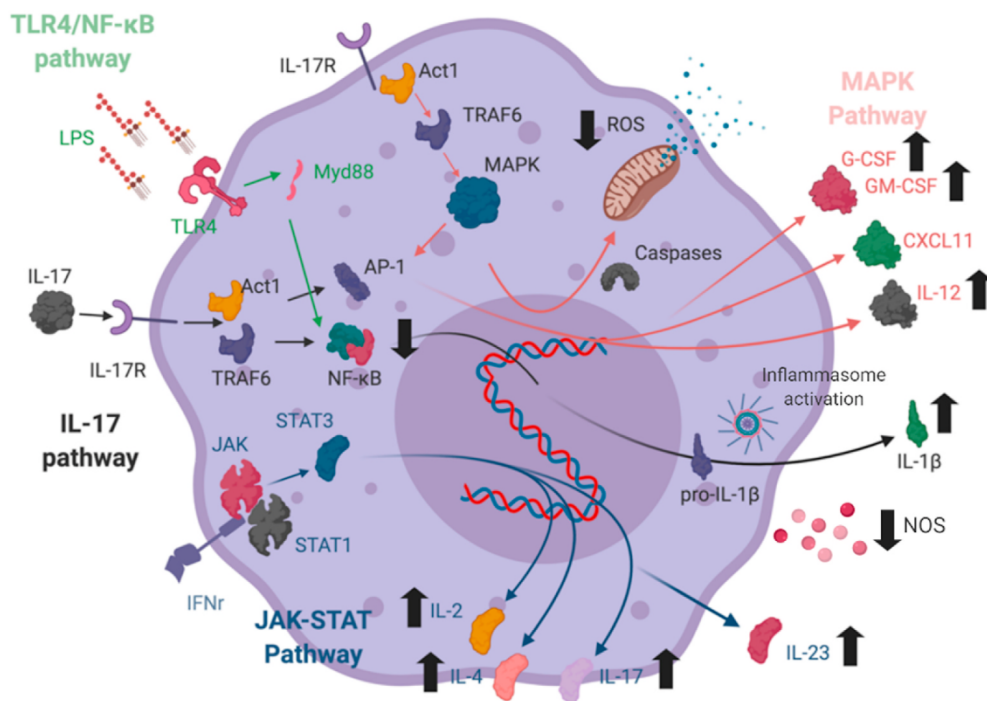


Fig. 6. Proposal of the main pro-inflammatory pathways modulated by DM-F2. The graphic was generated with [BioRender.com](#). Black arrows show the direct involvement of DM-F2 in the selected biochemical markers, proteins, and pathways.

paper, Other contribution.

Declaration of competing interest

The authors declare that they have no known competing financial interests or personal relationships that could have appeared to influence the work reported in this paper.

Acknowledgments

Author Martín Samuel Hernández Zazueta acknowledges Consejo Nacional de Ciencia y Tecnología (CONACyT-Mexico) for Ph.D. scholarship and the granted financial support for the projects 241133 and 2174. The technical support for this research work, provided by Edgar Sandoval-Petris, Juan Manuel Martínez-Soto, and María del Carmen Candia-Plata is also well appreciated.

Appendix A. Supplementary data

Supplementary data to this article can be found online at <https://doi.org/10.1016/j.fct.2021.112119>.

References

- Allavena, P., Garlanda, C., Borrello, M.G., Sica, A., Mantovani, A., 2008. Pathways connecting inflammation and cancer. *Curr. Opin. Genet. Dev.* 18, 3–10. <https://doi.org/10.1016/j.gde.2008.01.003>.
- Almeida, D., Domínguez-Pérez, D., Matos, A., Agüero-Chapin, G., Osorio, H., Vasconcelos, V., Campos, A., Antunes, A., 2020. Putative antimicrobial peptides of the posterior salivary glands from the cephalopod *Octopus vulgaris* revealed by exploring a composite protein database. *Antibiotics* 9, 757. <https://doi.org/10.3390/antibiotics9110757>.
- Ammendola, M., Haponska, M., Balik, K., Modrakowska, P., Matulewicz, K., Kazmierski, L., Lis, A., Kozlowska, J., Garcia-Valls, R., Giamberini, M., Bajek, A., Tylkowski, B., 2020. Stability and anti-proliferative properties of biologically active compounds extracted from *Cistus L.* after sterilization treatments. *Sci. Rep.* 10, 6521. <https://doi.org/10.1038/s4198-020-63444-3>.
- Balzano, M., Pacetti, D., Lucci, P., Fiorini, D., Frega, N.G., 2017. Bioactive fatty acids in mantis shrimp, crab and caramote prawn: their content and distribution among the main lipid classes. *J. Food Compos. Anal.* 59, 88–94. <https://doi.org/10.1016/j.jfca.2017.01.013>.
- Barzkar, Tamadoni Jahromi, Poorsaheli, Vianello, 2019. Metabolites from marine microorganisms, micro, and macroalgae: immense scope for pharmacology. *Mar. Drugs* 17, 464. <https://doi.org/10.3390/MD17080464>.
- Bray, F., Ferlay, J., Soerjomataram, I., 2018. Global Cancer Statistics 2018 : GLOBOCAN estimates of incidence and mortality worldwide for 36 cancers in 185 countries. *CA A Cancer J. Clin.* 1–31. <https://doi.org/10.3322/caac.21492>, 00.
- Brüne, B., Zhou, Y., Von Knethen, A., 2003. Nitric oxide, oxidative stress, and apoptosis. *Kidney Int. Suppl.* 63, S22–S24. <https://doi.org/10.1046/j.1523-1755.63.s84.6.x>.
- Changlong, L., Shen, H., Beixing, L., 1999. The immuno-stimulating activations of squid ink and its extracts. *Chin. J. Mar. Drugs* 18, 32–34.
- Chávez-Sánchez, L., Chávez-Rueda, K., Legorreta-Haquet, M., Zenteno, E., Ledesma-Soto, Y., Montoya-Díaz, E., Tesoro-Cruz, E., Madrid-Miller, A., Blanco-Favela, F., 2010. The activation of CD14, TLR4, and TLR2 by mMLDL induces IL-1 β , IL-6, and IL-10 secretion in human monocytes and macrophages. *Lipids Health Dis.* 9, 117. <https://doi.org/10.1186/1476-511X-9-117>.
- Chen, Y., Liu, H., Huang, H., Ma, Y., Wang, R., Hu, Y., Zheng, X., Chen, C., Tang, H., 2020. Squid ink polysaccharides protect human fibroblast against oxidative stress by regulating NADPH oxidase and connexin43. *Front. Pharmacol.* 10, 1574. <https://doi.org/10.3389/fphar.2019.01574>.
- Coleman, M.L., Sahai, E.A., Yeo, M., Bosch, M., Dewar, A., Olson, M.F., 2001. Membrane blebbing during apoptosis results from caspase-mediated activation of ROCK I. *Nat. Cell Biol.* 3, 339–345. <https://doi.org/10.1038/35070009>.
- Coussens, L.M., Werb, Z., 2002. Inflammation and cancer. *Nature* 420, 860–867. <https://doi.org/10.1038/nature01322>.
- Derby, C.D., 2014. Cephalopod ink: production, chemistry, functions and applications. *Mar. Drugs* 12, 2700–2730. <https://doi.org/10.3390/MD12052700>.
- Ebada, S., Edrada, R.A., Lin, W., Proksch, P., 2008. Methods for isolation, purification and structural elucidation of bioactive secondary metabolites from marine invertebrates. *Nat. Protoc.* 3 (12), 1820–1831. <https://doi.org/10.1038/nprot.2008.182>. In this issue.
- Ebenezer, J.L., Gunapriya, R., Ranganathan, K., Ganesh, M.K., 2020. Biologically active compounds in *Sepia pharaonis* fish (Ehrenber, 1831) ink extract from Chennai seacoast isolated by gas chromatography. *Drug Invent. Today* 13, 90–94.
- Egwuagu, C.E., 2009. STAT3 in CD4+ T helper cell differentiation and inflammatory diseases. *Cytokine* 47, 149–156. <https://doi.org/10.1016/j.cyto.2009.07.003>.
- Fahmy, R., Soliman, A.M., 2013. In vitro antioxidant, analgesic and cytotoxic activities of *Sepia officinalis* ink and Coelatura aegyptiaca extracts. *Afr. J. Pharm. Pharmacol.* 7, 1512–1522. <https://doi.org/10.5897/AJPP2013.3564>.
- Freeman, B.A., Pekarova, M., Rubbo, H., Trostchansky, A., 2017. Electrophilic nitro-fatty acids: nitric oxide and nitrite-derived metabolic and inflammatory signaling mediators. In: Ignarro, L.J., Freeman, B.A. (Eds.), *Nitric Oxide*. Academic Press - Elsevier, pp. 213–229. <https://doi.org/10.1016/B978-0-12-804273-1.00016-8>.
- Gabay, C., Lamachia, C., Palmer, G., 2010. IL-1 pathways in inflammation and human diseases. *Nat. Rev. Rheumatol.* 6, 232–241. <https://doi.org/10.1038/nrrheum.2010.4>.
- Gasparian, M.E., Bychkov, M.L., Yagolovich, A.V., Kirpichnikov, M.P., Dolgikh, D.A., 2017. The effect of cisplatin on cytotoxicity of anticancer cytokine TRAIL and its receptor-selective mutant variant DR5-B1. *Dokl. Biochem. Biophys.* 477, 385–388. <https://doi.org/10.1134/S1607672917060114>.
- Gertman, I., Barshop, B.A., 2018. Promises and pitfalls of untargeted metabolomics. *J. Inherit. Metab. Dis.* 41, 355–366. <https://doi.org/10.1007/s10545-017-0130-7>.
- Girija, S., Priyadarshini, J.V., Suba, K.P., Hariprasad, G., Raghuraman, R., 2011. Isolation and characterization of Lolduvin-S: a novel antimicrobial protein from the ink of Indians squid *Loligo duvaucelii*. *Int. J. Curr. Res. Rev.* 3, 4–14.
- Girija, S., Priyadarshini, V., Pandi, S.K., Hariprasad, P., Raghuraman, R., 2012. Antibacterial effect of squid ink on ESBL producing strains of *Escherichia coli* and *Klebsiella pneumoniae*. *Indian J. Geo-Marine Sci.* 41, 338–343.
- Groner, B., von Manstein, V., 2017. Jak Stat signaling and cancer: opportunities, benefits and side effects of targeted inhibition. *Mol. Cell. Endocrinol.* 451, 1–14. <https://doi.org/10.1016/j.mce.2017.05.033>.
- Gu, Y.P., Yang, X.M., Duan, Z.H., Luo, P., Shang, J.H., Xiao, W., Tao, Y.X., Zhang, D.Y., Zhang, Y.B., Liu, H.Z., 2017. Inhibition of chemotherapy-induced apoptosis of testicular cells by squid ink polysaccharide. *Exp. Ther. Med.* 14, 5889–5895. <https://doi.org/10.3892/etm.2017.5342>.
- Guo-fang, D., Fang-fang, H., Zui-su, Y., Di, Y.U., Yong-fang, Y., 2011. Anticancer activity of an oligopeptide isolated from hydrolysates of *Sepia Ink*. *Chin. J. Nat. Med.* 9, 151–155. <https://doi.org/10.3724/SP.J.1009.2011.00151>.
- Hernández-Zazueta, M.S., García-Romo, J.S., Noguera-Artiaga, L., Luzardo-Ocampo, I., Carbonell-Barrachina, Á.A., Taboada-Antelo, P., Campos-Vega, R., Rosas-Burgos, E.C., Burboa-Zazueta, M.G., Ezquerro-Brauer, J.M., Martínez-Soto, J.M., Santacruz-Ortega, H., del, C., Burgos-Hernández, A., 2021. Octopus vulgaris ink extracts exhibit antioxidant, antimutagenic, cytoprotective, antiproliferative, and proapoptotic effects in selected human cancer cell lines. *J. Food Sci.* 1750–3841, 15591. <https://doi.org/10.1111/1750-3841.15591>.
- Herrera-Cazares, L.A., Ramírez-Jiménez, A.K., Wall-Medrano, A., Campos-Vega, R., Loarca-Piña, G., Reyes-Vega, M.L., Vázquez-Landaverde, P.A., Gaytán-Martínez, M., 2019. Untargeted metabolomic evaluation of mango bagasse and mango bagasse based confection under in vitro simulated colonic fermentation. *J. Funct. Foods* 54, 271–280. <https://doi.org/10.1016/J.JFF.2019.01.032>.
- IARC, 2018. Estimated number of new cancer cases in 2018 worldwide [WWW Document]. *Canc. Today*. <https://gco.iarc.fr/>. accessed 5.29.20.
- Kelley, N., Jeltema, D., Duan, Y., He, Y., 2019. The NLRP3 inflammasome: an overview of mechanisms of activation and regulation. *Int. J. Mol. Sci.* 20, 3328. <https://doi.org/10.3390/jims2013328>.
- Khalifa, S.A.M., Elias, N., Farag, M.A., Chen, L., Saeed, A., Hegazy, M.E.F., Moustafa, M.S., El-Wahed, A.A., Al-Mousawi, S.M., Musharraf, S.G., Chang, F.R., Iwasaki, A., Suenaga, K., Alajlani, M., Göransson, U., El-Seedi, H.R., 2019. Marine natural products: a source of novel anticancer drugs. *Mar. Drugs*. <https://doi.org/10.3390/MD17090491>.
- Kuriki, K., Hirose, K., Wakai, K., Matsuo, K., Ito, H., Suzuki, T., Hiraki, A., Saito, T., Iwata, H., Tatematsu, M., Tajima, K., 2007. Breast cancer risk and erythrocyte compositions of n-3 highly unsaturated fatty acids in Japanese. *Int. J. Canc.* 121, 377–385. <https://doi.org/10.1002/ijc.22682>.
- Lé Cao, K.A., Boitard, S., Besse, P., 2011. Sparse PLS discriminant analysis: biologically relevant feature selection and graphical displays for multiclass problems. *BMC Bioinf.* 12 <https://doi.org/10.1186/1471-2105-12-253>.
- Li, W., Fan, Ting, Zhang, Y., Fan, Te, Zhou, P., Niu, X., He, L., 2013. *Houttuynia cordata Thunb.* volatile oil exhibited anti-inflammatory effects in vivo and inhibited nitric oxide and Tumor Necrosis Factor-α production in LPS-stimulated mouse peritoneal macrophages in vitro. *Phyther. Res.* 27, 1629–1639. <https://doi.org/10.1002/ptr.4905>.
- Lichtenstern, C.R., Ngu, R.K., Shalapour, S., Karin, M., 2020. Immunotherapy, inflammation and colorectal cancer. *Cells* 9, 618. <https://doi.org/10.3390/cells9030618>.
- Liú, C., Li, X., Li, Y., Feng, Y., Zhou, S., Wang, F., 2008. Structural characterisation and antimutagenic activity of a novel polysaccharide isolated from *Sepiella maindroni* ink. *Food Chem.* 110, 807–813. <https://doi.org/10.1016/j.foodchem.2008.02.026>.
- Liu, H.-Z., Tao, Y.-X., Luo, P., Deng, C.-M., Gu, Y.-P., Yang, L., Zhong, J.-P., 2016a. Preventive effects of a novel polysaccharide from *Sepia esculenta* ink on ovarian failure and its action mechanisms in cyclophosphamide-treated mice. *J. Agric. Food Chem.* 64, 5759–5766. <https://doi.org/10.1021/acs.jafc.6b01854>.
- Liu, H.-Z., Xiao, W., Gu, Y.-P., Tao, Y.-X., Zhang, D.-Y., Du, H., Shang, J.-H., 2016b. Polysaccharide from *Sepia esculenta* ink and cisplatin inhibit synergistically proliferation and metastasis of triple-negative breast cancer MDA-MB-231 cells. *Iran. J. Basic Med. Sci.* 19, 1292–1298. <https://doi.org/10.22038/ijbms.2016.7913>.
- Lonkar, P., Dedon, P.C., 2011. Reactive species and DNA damage in chronic inflammation: reconciling chemical mechanisms and biological fates. *Int. J. Canc.* <https://doi.org/10.1002/ijc.25815>.
- Lord, R.M., Zegke, M., Henderson, I.R., Pask, C.M., Shepherd, H.J., McGowan, P.C., 2019. β -Ketoimino Iridium(III) organometallic complexes: selective cytotoxicity towards colorectal cancer cells HCT116 p53 -. *Chem. Eur. J.* 25, 495–500. <https://doi.org/10.1002/chem.201804901>.
- Lu, S., Zuo, T., Zhang, N., Shi, H., Liu, F., Wu, J., Wang, Y., Xue, C., Tang, Q., 2016. High throughput sequencing analysis reveals amelioration of intestinal dysbiosis by squid

- ink polysaccharide. *J. Funct. Foods* 20, 506–515. <https://doi.org/10.1016/j.jff.2015.11.017>.
- Luna-Vital, D., Weiss, M., Gonzalez de Mejia, E., 2017. Anthocyanins from purple corn ameliorated Tumor Necrosis Factor- α -induced inflammation and insulin resistance in 3T3-L1 adipocytes via activation of insulin signaling and enhanced GLUT4 translocation. *Mol. Nutr. Food Res.* 61, 1–13. <https://doi.org/10.1002/mnfr.201700362>.
- Luzardo-Ocampo, I., Campos-Vega, R., Cuellar-Nuñez, M.L.L., Vázquez-Landaverde, P.A., Mojica, L., Acosta-Gallegos, J.A.A., Loarca-Piña, G., 2018. Fermented non-digestible fraction from combined nixtamalized corn (*Zea mays* L.)/cooked common bean (*Phaseolus vulgaris* L.) chips modulate anti-inflammatory markers on RAW 264.7 macrophages. *Food Chem.* 259, 7–17. <https://doi.org/10.1016/j.foodchem.2018.03.096>.
- Luzardo-Ocampo, I., Campos-Vega, R., Gonzalez de Mejia, E., Loarca-Piña, G., 2020. Consumption of a baked corn and bean snack reduced chronic colitis inflammation in CD-1 mice via downregulation of IL-1 receptor, TLR, and TNF- α associated pathways. *Food Res. Int.* 132, 109097. <https://doi.org/10.1016/j.foodres.2020.109097>.
- Ma, C.S., Avery, D.T., Chan, A., Batten, M., Bustamante, J., Boisson-Dupuis, S., Arkwright, P.D., Kreins, A.Y., Averbuch, D., Engelhard, D., Magdoff, K., Kilic, S.S., Minegishi, Y., Nonoyama, S., French, M.A., Choo, S., Smart, J.M., Peake, J., Wong, M., Gray, P., Cook, M.C., Fulcher, D.A., Casanova, J.-L., Deenick, E.K., Tangye, S.G., 2012. Functional STAT3 deficiency compromises the generation of human T follicular helper cells. *Blood* 119, 3997–4008. <https://doi.org/10.1182/blood-2011-11-392985>.
- Madaras, F., Gerber, J.P., Peddie, F., Kokkinn, M.J., 2010. The effect of sampling methods on the apparent constituents of ink from the squid *Sepioteuthis australis*. *J. Chem. Ecol.* 36, 1171–1179. <https://doi.org/10.1007/s10886-010-9869-0>.
- Malve, H., 2016. Exploring the ocean for new drug developments: marine pharmacology. *J. Pharm. BioAllied Sci.* <https://doi.org/10.4103/0975-7406.171700>.
- Maselli, V., Galdiero, E., Salzano, A.M., Scaloni, A., Maione, A., Falanga, A., Naviglio, D., Guida, M., Di Cosmo, A., Galdiero, S., 2020. OctoPartenopin: identification and preliminary characterization of a novel antimicrobial peptide from the suckers of *Octopus vulgaris*. *Mar. Drugs* 18, 380. <https://doi.org/10.3390/md18080380>.
- Mitchison, T.J., 2012. The proliferation rate paradox in antimitotic chemotherapy. *Mol. Biol. Cell* <https://doi.org/10.1091/mbc.E10-04-0335>.
- Mysuru Shivanna, L., Urooj, A., 2016. A review on dietary and non-dietary risk factors associated with gastrointestinal cancer. *J. Gastrointest. Canc.* 47, 247–254. <https://doi.org/10.1007/s12029-016-9845-1>.
- Naraoka, T., Chung, H.-S.S., Uchisawa, H., Sasaki, J.I., Matsue, H., 2000. Tyrosinase activity in antitumor compounds of squid ink. *Food Sci. Technol. Res.* 6, 171–175. <https://doi.org/10.3136/fstr.6.171>.
- Noguera-Artiaga, L., Salvador, M.D., Fregapane, G., Collado-González, J., Wojdylo, A., López-Lluch, D., Carbonell-Barrachina, Á.A., 2019. Functional and sensory properties of pistachio nuts as affected by cultivar. *J. Sci. Food Agric.* 99, 6696–6705. <https://doi.org/10.1002/jsfa.9951>.
- Oh, Y.T., Lee, J.Y., Lee, J., Lee, J.H., Kim, J.-E., Ha, J., Kang, I., 2010. Oleamide suppresses lipopolysaccharide-induced expression of iNOS and COX-2 through inhibition of NF- κ B activation in BV2 murine microglial cells. *Neurosci. Lett.* 474, 148–153. <https://doi.org/10.1016/j.neulet.2010.03.026>.
- Pencik, J., Pham, H.T.T., Schmoellerl, J., Javaheri, T., Schleiderer, M., Culig, Z., Merkel, O., Moriggl, R., Grebien, F., Kenner, L., 2016. JAK-STAT signaling in cancer: from cytokines to non-coding genome. *Cytokine* 87, 26–36. <https://doi.org/10.1016/j.cyto.2016.06.017>.
- Rajamäki, K., Lappalainen, J., Öörni, K., Välimäki, E., Matikainen, S., Kovanan, P.T., Eklund, K.K., 2010. Cholesterol crystals activate the NLRP3 inflammasome in human macrophages: a novel link between cholesterol metabolism and inflammation. *PLoS One* 5, e11765. <https://doi.org/10.1371/journal.pone.0011765>.
- RoyChoudhury, S., More, T.H., Chattopadhyay, R., Lodh, I., Ray, C.D., Bose, G., Sarkar, H.S., Chakravarty, B., Rapole, S., Chaudhury, K., 2017. Polycystic ovary syndrome in Indian women: a mass spectrometry based serum metabolomics approach. *Metabolomics* 13, 115. <https://doi.org/10.1007/s11306-017-1253-4>.
- Russo, G.L., De Nisco, E., Fiore, G., Di Donato, P., D'Ischia, M., Palumbo, A., D'Ischia, M., Palumbo, A., 2003. Toxicity of melanin-free ink of *Sepia officinalis* to transformed cell lines: identification of the active factor as tyrosinase. *Biochem. Biophys. Res. Commun.* 308, 293–299. [https://doi.org/10.1016/S0006-291X\(03\)01379-2](https://doi.org/10.1016/S0006-291X(03)01379-2).
- Santos, S., Oliveira, A., Lopes, C., 2013. Systematic review of saturated fatty acids on inflammation and circulating levels of adipokines. *Nutr. Res.* 33, 687–695. <https://doi.org/10.1016/j.nutres.2013.07.002>.
- Sarkar, D., Fisher, P.B., 2006. Molecular mechanisms of aging-associated inflammation. *Canc. Lett.* 236, 13–23. <https://doi.org/10.1016/j.canlet.2005.04.009>.
- Setterrrahmane, S., Xu, H., 2017. Tumor-related interleukins: old validated targets for new anti-cancer drug development. *Mol. Canc.* 16, 153. <https://doi.org/10.1186/s12943-017-0721-9>.
- Sohail, M.F., Rehman, M., Sarwar, H.S., Naveed, S., Qureshi, O.S., Bukhari, N.I., Hussain, I., Webster, T.J., Shahnaz, G., 2018. Advancements in the oral delivery of Docetaxel: challenges, current state-of-the-art and future trends. *Int. J. Nanomed.* Volume 13, 3145–3161. <https://doi.org/10.2147/IJN.S164518>.
- Soufi-Kechau, E., Sariya, I., Bezaa, A., Marrakchi, N., El Ayeb, M., 2017. Antitumoral activity inks of *Sepia officinalis* and *Octopus vulgaris* (Cephalopoda) from the northern tunisian coast (central Mediterranean sea). *Ann. Ser. Hist. Nat.* 27, 125–136. <https://doi.org/10.19233/ASHN.2017.15>.
- Sun, L., Zhang, L., Yu, J., Zhang, Y., Pang, X., Ma, C., Shen, M., Ruan, S., Wasan, H.S., Qiu, S., 2020. Clinical efficacy and safety of anti-PD-1/PD-L1 inhibitors for the treatment of advanced or metastatic cancer: a systematic review and meta-analysis. *Sci. Rep.* 10, 2083. <https://doi.org/10.1038/s41598-020-58674-4>.
- Taylor, W.F., Moghadam, S.E., Moridi Farimani, M., N, Ebrahimi, S., Tabefam, M., Jabbarzadeh, E., 2019. A multi-targeting natural compound with growth inhibitory and anti-angiogenic properties re-sensitizes chemotherapy resistant cancer. *PLoS One* 14, e0218125. <https://doi.org/10.1371/journal.pone.0218125>.
- Troncone, L., De Lisa, E., Bertapelle, C., Porcellini, A., Laccetti, P., Polese, G., Di Cosmo, A., 2015. Morphofunctional characterization and antibacterial activity of haemocytes from *Octopus vulgaris*. *J. Nat. Hist.* 49, 1457–1475. <https://doi.org/10.1080/00222933.2013.826830>.
- Trott, O., Olson, A.J.A., 2010. AutoDock Vina: improving the speed and accuracy of docking with a new scoring function, efficient optimization, and multithreading. *J. Comput. Chem.* 31, 455–461. <https://doi.org/10.1002/jcc.21334>.
- Tuomisto, A.E., Mäkinen, M.J., Väyrynen, J.P., 2019. Systemic inflammation in colorectal cancer: underlying factors, effects, and prognostic significance. *World J. Gastroenterol.* 25, 4383–4404. <https://doi.org/10.3748/wjg.v25.i31.4383>.
- Van Vuuren, R.J., Botes, M., Jurgens, T., Joubert, A.M., Van Den Bout, I., 2019. Novel sulphamoylated 2-methoxy estradiol derivatives inhibit breast cancer migration by disrupting microtubule turnover and organization. *Canc. Cell Int.* 19 <https://doi.org/10.1186/s12935-018-0719-4>.
- von Mering, C., Jensen, L.J., Kuhn, M., Chaffron, S., Doerks, T., Kruger, B., Snel, B., Bork, P., Krüger, B., Snel, B., Bork, P., 2007. STRING 7 – recent developments in the integration and prediction of protein interactions. *Nucleic Acids Res.* 35, 358–362. <https://doi.org/10.1093/nar/gkl825>.
- Wang, S., Wu, D., Lamont-Fava, S., Matthan, N.R., Honda, K.L., Lichtenstein, A.H., 2009. In vitro fatty acid enrichment of macrophages alters inflammatory response and net cholesterol accumulation. *Br. J. Nutr.* 102, 497. <https://doi.org/10.1017/S0007114509231758>.
- Wargasetti, T.L., Widodo, N., 2019. The link of marine products with autophagy-associated cell death in cancer cell. *Curr. Pharmacol. Reports* 5, 35–42. <https://doi.org/10.1007/s40495-019-00167-8>.
- Weng, S., Mao, L., Gong, Y., Sun, T., Gu, Q., 2017. Role of quercetin in protecting ARPE-19 cells against H2O2-induced injury via nuclear factor erythroid 2 like 2 pathway activation and endoplasmic reticulum stress inhibition. *Mol. Med. Rep.* 16, 3461–3468. <https://doi.org/10.3892/mmr.2017.6964>.
- Yuan, B.Z., Jefferson, A.M., Millicchia, L., Popescu, N.C., Reynolds, S.H., 2007. Morphological changes and nuclear translocation of DLC1 tumor suppressor protein precede apoptosis in human non-small cell lung carcinoma cells. *Exp. Cell Res.* 313, 3868–3880. <https://doi.org/10.1016/j.yexcr.2007.08.009>.
- Zhang, Z., Li, Y., Lin, B., Schroeder, M., Huang, B., 2011. Identification of cavities on protein surface using multiple computational approaches for drug binding site prediction. *Bioinformatics* 27, 2083–2088. <https://doi.org/10.1093/bioinformatics/btr331>.
- Zhang, Z., Sun, L., Zhou, G., Xie, P., Ye, J., 2017. *Sepia* ink oligopeptide induces apoptosis and growth inhibition in human lung cancer cells. *Oncotarget* 8, 23202–23212. <https://doi.org/10.18632/oncotarget.15539>.
- Zhong, J.-P., Wang, G., Shang, J.-H., Pan, J.-Q., Li, K., Huang, Y., Liu, H.-Z., 2009. Protective effects of squid ink extract towards hemopoietic injuries induced by cyclophosphamide. *Mar. Drugs* 7, 9–18. <https://doi.org/10.3390/md7010009>.
- Zuo, T., Cao, L., Sun, X., Li, X., Wu, J., Lu, S., Xue, C., Tang, Q., 2014. Dietary squid ink polysaccharide could enhance SIgA secretion in chemotherapeutic mice. *Food Funct.* 5, 3189–3196. <https://doi.org/10.1039/C4FO00569D>.